Depth of the Stable Atmospheric Boundary Layer over a Shallow Uniform Slope

Andrew James MAGUIRE[1], Julia Margaret REES[2] and Stephen Hal DERBYSHIRE[3]

[1] Department of Applied Mathematics, The University of Sheffield,
Hicks Building, Hounsfield Road, Sheffield, S3 7RH, U.K.
[2] Corresponding author: J. M. Rees, j.rees@shef.ac.uk,
Tel: 44 (0) 114 2223782, FAX: 44 (0) 114 2223739
[3] The Meteorological Office, FitzRoy Road, Exeter, Devon, EX1 3PB, U.K.

(Received 14 May 2007; received in revised form 13 June 2007; accepted 15 June 2007)

ABSTRACT
This paper is concerned with the depth of the stably stratified atmospheric boundary layer overlying a shallow uniform slope. A specified surface heat flux is applied. Large eddy simulation modelling is used to compare the boundary layer depths predicted by three different definitions for the depth of the stable layer that are in common use: the height at which the heat flux has dropped to 5% of its surface value, the height at which the Zilitinkevich ratio is a prescribed constant value, and, thirdly, the height at which the wind speed reaches its maximum value. These three definitions are based on different physical properties. Results from both one-dimensional (in the sense that span-wise spatial derivatives are all assumed to be zero but the three components of the velocity field are included) and fully three-dimensional simulations are presented. Key findings from this study indicate that in the one-dimensional simulations, cross-slope winds could adversely affect the surface layer statistics leading to the prediction of an overly shallow boundary layer. This problem was alleviated in the three-dimensional simulations. This suggests that fully three-dimensional simulations are required for stable boundary layers over sloping terrain.
Key words: Stable atmospheric boundary layer, sloping terrain, large eddy simulations, boundary layer depth.

Altura de la Capa Límite Atmosférica Estable sobre una Pendiente Homogéna Somera

RESUMEN
Este trabajo está relacionado con la altura de una capa límite atmosférica establemente estratificada sobre una pendiente homogéna somera. Se aplica un determinado flujo de calor superficial. Se utiliza simulación numérica de grandes remolinos (LES) para comparar las alturas de capa límite pronosticadas por tres diferentes definiciones de altura de capa estable que habitualmente se utilizan: la altura a la cual el flujo de calor ha disminuido a un 5% de su valor superficial, la altura a la cual la razón de Zilitinkevich es un valor prescrito constante, y en tercer lugar la altura a la que la velocidad del viento alcanza su valor máximo. Estas tres definiciones se basan en diferentes propiedades físicas. Se presentan los resultados tanto de las simulaciones unidimensionales (en el sentido de que las derivadas espaciales transversales son cero pero se incluyen las tres componentes de la velocidad) como de las tridimensionales. Los resultados fundamentales de este estudio señalan que en las simulaciones unidimensionales los vientos transversales a la pendiente podían afectar negativamente a

las estadísticas de la capa superficial, dando lugar a la predicción de una capa límite demasiado somera. Este problema fue atenuado en las simulaciones tridimensionales. Esto sugiere que se necesitan simulaciones tridimensionales para capas límites estables sobre terreno en pendiente.
Palabras clave: capa límite atmosférica estable, terreno en pendiente, simulaciones de grandes remolinos (LES), altura de capa límite.

INTRODUCTION

The stably stratified (or nocturnal) atmospheric boundary layer (SBL) can arise due to the radiative cooling that takes place at nighttime. It is less well understood than its convective (daytime) counterpart. There are several reasons for this. Whilst the convective boundary layer (CBL) is relatively insensitive to even moderate scale topography (Kaimal et al. 1982), the dynamics and structure of the SBL are influenced by even small-scale topographic features (Derbyshire and Wood 1994). For example, a shallow slope with a gradient of the order of 1:1000 can affect the surface buoyancy fluxes, and also wind and temperature profiles across the whole boundary layer (Maguire et al. 2006). At mid-latitudes the SBL tends to be short lived due to the effects of diurnal variations, thus in order to study the well-developed SBL free from the complicating effects of diurnal variations, several observational campaigns have been run in polar regions where the nocturnal boundary layer may persist over much longer periods during the months of winter darkness. Even though the ice shelves around Antarctica at first sight might seem to present an ideal natural laboratory for making observational studies of the SBL, it has been found that the gentle slopes of an ice shelf down towards the coast can influence the physics of the SBL (King 1990; Kottmeier 1986; Handorf et al. 1999). Mahrt et al. (2001) demonstrated that regions previously considered too flat and windy for the development of significant slope flows (e.g. Kansas U.S.A.) can in fact host extremely shallow near-surface flows that influence surface exchange processes. Due to the shallowness of the SBL it is typically poorly resolved in weather forecasting and climate prediction models. In order to account for slope flow transport of the SBL in mesoscale models we need either specialized boundary layer parameterization schemes, or very high vertical resolution near the ground which can be computationally expensive (Skyllingstad 2003). Skyllingstad used a large eddy simulation model with rotated coordinates and an open boundary to simulate katabatic flows over sloping terrain with steep gradients of 1:5 and shallower gradients of 1:100. He found that even gentle slopes can lead to significant drainage winds and can effectively prevent the formation of very stable layers.

The purpose of this paper is to use large eddy simulation modelling to investigate the depth of the SBL over very shallow slopes with gradients of 1:500 and 1:1000. Such slopes are found in the ice shelves of Antarctica and in the planes of Kansas. Different definitions for obtaining the depth of the SBL are compared and the orientation of the wind to the slope is considered. The large eddy simulation model is described in section 2 and results from both one-dimensional (1D) and three-dimensional (3D) simulations are presented in section 3. Conclusions are summarized in section 4.

2. THE LARGE EDDY SIMULATION MODEL

In the SBL length scales vary from small scale turbulent eddies to large scale motions of the order of the depth of the boundary layer. In order to resolve the smallest scale motions a very fine grid mesh would be required. Solution of the Navier-Stokes (NS) equations on such a grid would be highly impractical due to both the amount of memory storage required and the time required for the computations. Thus a direct numerical simulation (DNS) is not feasible. The idea behind the technique of large eddy simulation (LES) is to circumvent these physical restrictions by computing the smaller scale subgrid processes through the use of a simple parameterization. Values of field variables at grid points represent their (ensemble) average over a grid volume.

In this paper we use a LES model to simulate the evolution of the SBL over a shallow uniform slope. The FORTRAN code for the study was provided by the U.K. Meteorological Office. Details of the model can be found in Mason (1989) and Mason and Derbyshire (1990). However, for completeness a brief outline of the model is given here. For this study modifications were made to incorporate the sloping surface.

A schematic of the co-ordinate system used is shown in Fig. 1. In a frame of reference where $x = (x_1, x_2, x_3) = (x, y, z)$ are the ordinates, the x-axis is aligned in the direction of the surface wind.

The general equations which govern the flow of the atmosphere are the NS momentum equations, the continuity equation and the equation for conservation of

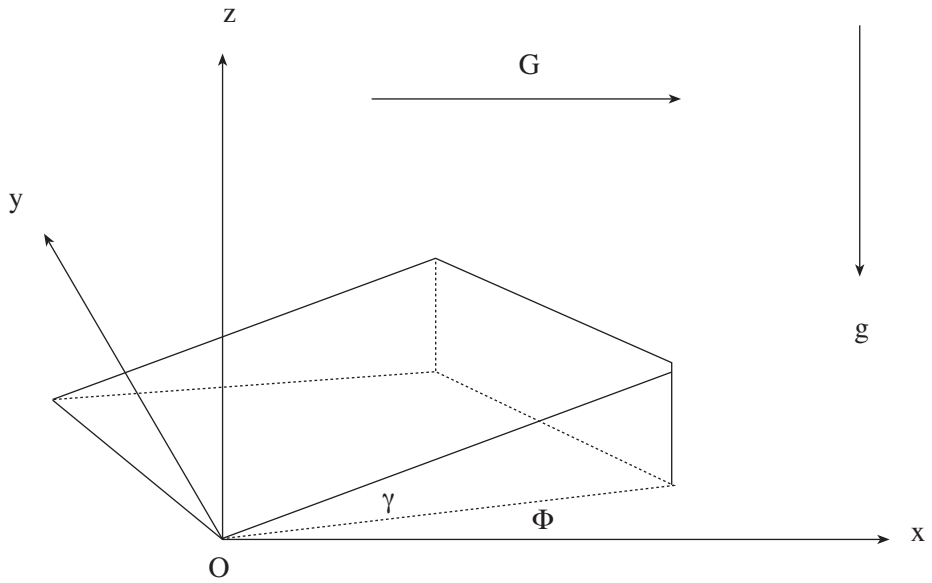

Figure 1.- Schematic diagram showing the orientation of the slope with respect to the *(x, y, z)* co-ordinate system. The gradient of the slope is γ. The slope is rotated through an angle $\phi = 0°$ with respect to the x-axis. corresponds to the upslope direction of 0°. The geostrophic wind, magnitude G, acts parallel to the *x, y*- plane (the direction shown is arbitrary).

heat. As the NS equations are strongly nonlinear and the wind velocity can exhibit large vertical gradients across shallow layers, a Reynolds averaging procedure is used to solve these equations in order to overcome numerical difficulties. This procedure splits the velocity into two components, $u_i = \bar{u}_i + u'_i$, the first being the mean wind, $\bar{u}_i$, and the second representing the random fluctuations, u'_i. Using the Boussinesq approximation where density variations are assumed to be negligible except in the buoyancy term, the Reynolds averaged momentum equations for flow over a sloping surface can be expressed as

$$\frac{\partial \bar{u}_i}{\partial t} + \bar{u}_j \frac{\partial \bar{u}_i}{\partial x_j} = - \frac{1}{\rho} \frac{\partial \bar{p}}{\partial x_i} + g\delta_{13} \frac{\theta'}{\theta_{ref}} + (1-\delta_{i3})\, g\gamma \frac{\theta'}{\theta_{ref}} e^{i\phi} + \\ + f\varepsilon_{ij3}\bar{u}_j + \upsilon_{air} \frac{\partial^2 \bar{u}_i}{\partial x_j^2} - \frac{\partial \tau_{ij}}{\partial x_j}, \tag{1}$$

where,

$\boldsymbol{u} = (u_1, u_2, u_3) = (u, v, w)$ is the wind velocity vector,
ρ is the density of the fluid,
p denotes pressure,
g is the acceleration due to gravity,
f is the Coriolis parameter,
θ_{ref} is a reference potential temperature, taken to be 300 K,
θ' denotes fluctuations of potential temperature, θ, *i.e.* $\theta' = \theta - \theta_{ref}$,
υ_{air} is the viscosity of air,
δ_{ij} is the Kronecker delta,
$\tau_{ij} = \overline{u'_i u'_j}$ is the Reynolds stress tensor

and

ε_{ijk} is the alternating pseudo tensor.

We used both 1D (in the sense that spanwise spatial derivatives are all assumed to be zero but the three components of the velocity field are included) and fully 3D numerical simulations in order to investigate long term time effects of the orientation and magnitude of a sloping surface on the depth of the SBL. The NS equations were evaluated using a grid which has constant grid spacing in the *x*- and *y*- directions and a stretched grid in the vertical. The stability of the finite difference schemes used in the LES code was ensured through the use of a viscous stability criterion, viz. the Courant-Fredericks-Lewy criterion for advection and a weak time filter. The quadratic energy conserving scheme of Piacsek and Williams (1970) was applied. The subgrid scale backscatter scheme of Brown et al. (1994) was used.

2.1. 1D SIMULATIONS

Eight runs were made to simulate flow over a shallow slope of 1:1000. The slope was considered fixed and orientated such that the upslope direction was 0°. The direction of the geostrophic wind relative to the slope was incremented by 45° in each successive run. Thus, the 90° case corresponds to the geostrophic wind aligned at 90° anti-clockwise to the upslope direction of 0° (see Fig. 1). For comparison a flat terrain simulation was also performed. Standard parameter values were used in all the simulations as given in Table 1.

Table 1.- Definition of model parameters

Quantity	Symbol	Value
Mixing length	l_0	40 m
Surface roughness length	z_0	0.01 m
Geostrophic wind	U_g	10 m s^{-1}
Critical flux Richardson no.	R_{fc}	0.25
Prandtl no.	Pr	0.7

As the SBL is relatively shallow, the vertical domain extended to 1000 m above the surface. To check that the model had sufficient resolution, some initial runs with a slope of 1:1000 were compared using different vertical resolutions until consistency was obtained. The vertical resolution used varied with height and had more grid points near to the surface due to the larger shear experienced there. A total of 200 grid points in the vertical were used. Grid points closest to the ground were separated by 0.24 m. The resolution at the top of the domain was around 9.4 m. 47 grid points covered the first 100 m above the surface. Initial values for the horizontal wind components were obtained by integrating the neutral boundary for 18000 s. By that time, the boundary layer had reached steady state. Surface cooling of either 15 Wm^{-2}, or 30 Wm^{-2}, was applied and the model was integrated until a total integration time of 32400 s (i.e. 9 hours) was reached.

2.2. 3D SIMULATIONS

As in the 1D simulations, a neutral boundary layer was first simulated over an integration time of 18000 s. This provided the initial conditions for all the subsequent stable runs. Each run was integrated with surface cooling applied for about 4 hours. This is a shorter time than that considered in the 1D simulations due to the extra CPU time required for 3D runs. The computational domain comprised 54 x 40 x 40 grid points. The distance between the lowest few vertical grid points was of the order of 2 m. Twenty four grid points covered the lowest 300 m. A

number of runs with a higher vertical grid resolution were performed in order to check for grid dependency. Good compatibility was found.

3. RESULTS

3.1. DEFINITIONS OF BOUNDARY LAYER HEIGHT

Currently there exists controversy over which is the best way to measure the depth of the SBL. Three of the most commonly used definitions are based on different physical properties of the SBL. These are:

(a) The height at which the heat flux has fallen to 5% of its surface value. For the simulations presented herein, the value of the surface heat flux is prescribed.

(b) A measure of the depth of the SBL can be determined from the Zilitinkevich ratio, $h = Zi\sqrt{\frac{u_* L}{f}}$, where Zi is Zilitinkevich's constant, u_* is the friction velocity, L is the Monin-Obukhov length scale and f is the Coriolis parameter (Zilitinkevich 1972). In this definition h is based on surface layer quantities. In this study we took $Zi = 0.4$.

(c) The height at which the wind speed reaches its maximum value $|W|_{max}$.

Henceforth we will refer to these definitions as the 5% method, the Zi method and the $|W|_{max}$ method respectively.

3.2. 1D SIMULATIONS

First of all we will consider results from the 1D simulations. Tables 2 and 3 compare results from simulations with an applied surface cooling of 15 Wm^{-2}, applied over sloping surface of 1:1000 and 1:500 respectively. Using the 5% method it can be seen that the slopes with orientations of 0°, 45°, 270° and 315° develop deeper boundary layers when the slope magnitude is doubled. Slopes with orientations of 90°, 135°, 180° and 225° develop shallower boundary layers. However, when the Zi method is used, slopes orientated at 180°, 225°, 270° and 315° have larger boundary layer depths when the slope magnitude is doubled, whilst orientations of 0°, 45°, 90° and 135° correspond to shallower boundary layers.

The variation of the boundary layer depth with slope orientation exhibits a pattern that is independent of slope magnitude. The 5% method indicates that the shallowest boundary layer is associated with a slope orientation of 135°, whilst the deepest boundary layer occurs for a slope direction of 315°. For the Zi method the 45° case has the least depth and the largest occurs when the slope direction is 225°.

Table 2.- This table shows the boundary layer heights in metres from the 1D model with a slope of 1:1000, and an applied surface cooling of 15 Wm^{-2} calculated using (a) the 5% method, (b) the *Zi* method and (c) the $|W|_{max}$ method, after a total integration time of 32400 s.

Method	No slope	0°	45°	90°	135°	180°	225°	270°	315°
5%	292.1	297.5	292.7	287.2	284.8	286.5	291.6	296.8	299.4
Zi	309.5	302.2	294.7	296.0	305.4	317.2	324.3	322.9	313.8
$\|W\|_{max}$	319.6	328.9	328.9	319.6	319.6	319.6	319.6	319.6	328.9

Table 3.- As for Table 2 but with a slope with a gradient of 1:500, and an applied cooling of 15 Wm^{-2} after a total integration time of 32400 s.

Method	No slope	0°	45°	90°	135°	180°	225°	270°	315°
5%	292.1	303.5	293.3	282.5	277.5	281.3	291.2	301.8	306.8
Zi	309.5	295.1	279.9	282.3	301.4	325.1	339.1	336.1	318.2
$\|W\|_{max}$	319.6	338.1	328.9	319.6	310.4	310.4	319.6	328.9	338.1

Table 4.- As for Table 2 but with a slope with a gradient of 1:500, and an applied cooling of 15 Wm^{-2} after a total integration time of 32400 s.

Method	No slope	0°	45°	90°	135°	180°	225°	270°	315°
5%	292.1	303.5	293.3	282.5	277.5	281.3	291.2	301.8	306.8
Zi	309.5	295.1	279.9	282.3	301.4	325.1	339.1	336.1	318.2
$\|W\|_{max}$	319.6	338.1	328.9	319.6	310.4	310.4	319.6	328.9	338.1

Results from 1D simulations where the heat flux was doubled to 30 Wm^{-2} are presented in Table 4. This is a relatively large surface heat flux but is typical of those occurring during the winter months over an Antarctic ice shelf (Rees 1991). An immediate observation is that the boundary layer depth is much shallower than for those described in Tables 2 and 3, from which we can conclude that doubling the surface cooling effects the boundary layer depth more dramatically than doubling the magnitude of the slope. Minimum and maximum boundary layer depths now occur for 90° and 270° respectively, compared with 135° and 315° for a cooling rate of 15 Wm^{-2}. Of particular note is the apparent anomaly that occurs for the slope orientation of 90° in both the 5% and *Zi* methods. For this cross-slope wind direction the Obukhov length is relatively large and hence surface layer quantities are particularly sensitive to this parameter.

Boundary layer depths predicted by the measure $|W|_{max}$ show greater variation with slope orientation as the slope magnitude is increased. Further, since this measure is not directly based on surface layer statistics, we do not observe the anomaly that occurs for orientations of 90° when strong surface cooling is applied (see Table 4).

3.3. 3D SIMULATIONS

The statistics in Table 5 are derived from 3D simulations using a slope of magnitude 1:1000. Similarly, Table 6 contains results from 3D simulations for a slope of 1:500. For the case of the shallower slope, the predicted boundary layer depth is greatest for the $|W|_{max}$ method, intermediate for the *Zi* method and least for the 5% method across all wind directions. This pattern is almost maintained when the slope gradient is doubled (Table 6), except that the depths predicted by the 5% method for wind directions of 180° and 270° are now greater than those derived from the $|W|_{max}$ method. However, it should be noted that as the wind speed does not change much with height in the vicinity where its maximum value occurs, the $|W|_{max}$ method is not necessarily an accurate indicator of boundary layer depth. Note that the boundary layer depths are generally deeper than those presented in the results from the 1D simulations - this is because the total integration time was reduced in 3D due to the increased computing resources needed.

Doubling the surface cooling rate to 30 Wm^{-2} causes a decrease in the predicted boundary layer depth (see Table 7) compared to the results given in Table 5 for a cooling rate of 15 Wm^{-2}. However, the decrease is substantially greater for the 5% and *Zi* methods than for the $|W|_{max}$ method. This is because these methods are more sensitive to surface values.

Tables 5, 6 and 7 indicate that the 3D model copes better than the 1D model for resolving cross-slope winds. The anomalous boundary layer depths which were most marked using the 5% and *Zi* methods for a wind direction of 90° were not observed in the 3D simulations. This suggests that fully 3D simulations are ideally required for studies of the SBL over sloping terrain.

Table 5.- This table shows the boundary layer heights in metres from the 3D model with a slope of 1:1000, and an applied surface cooling of 15 Wm^{-2} calculated using (a) the 5% method, (b) the *Zi* method and (c) the $|W|_{max}$ method, after a total integration time of 27900 s.

Method	No slope	0°	90°	180°	270°
5%	376.8	378.8	393.6	383.2	370.2
Zi	344.2	324.6	333.9	356.5	344.1
$\|W\|_{max}$	393.1	393.1	412.4	393.1	393.1

Table 6.- As for Table 5 but with a slope with a gradient of 1:500, and an applied cooling of 15 Wm^{-2} after a total integration time of 27900 s.

Method	No slope	0°	90°	180°	270°
5%	376.9	381.3	376.6	384.1	392.0
Zi	344.2	331.2	337.7	355.4	366.0
$\|W\|_{max}$	393.1	393.1	377.1	377.1	377.1

Table 7.- As for Table 5 but with a slope with a gradient of 1:1000, and an applied cooling of 30 Wm^{-2} after a total integration time of 27900 s.

Method	No slope	0°	90°	180°	270°
5%	213.7	219.1	207.4	199.6	214.1
Zi	182.4	173.1	163.4	191.8	197.4
$\|W\|_{max}$	267.9	278.0	288.2	267.9	267.9

4. CONCLUSIONS

In this paper we have used large eddy simulation modelling to investigate the depth of the SBL overlying an inclined surface subtending a small angle with the horizontal. Slopes with gradients of 1:500 and 1:1000 were investigated. The effect of surface cooling on the boundary depth was also investigated, as was the wind direction in relation to the orientation of the slope.

It was found that doubling the magnitude of the applied surface cooling effects the boundary layer depth more significantly than doubling the gradient of the slope. When comparing the boundary layer height using the 5% and *Zi* methods with imposed surface cooling of 15 Wm^{-2} or 30 Wm^{-2}, significant variation with slope direction was observed in both the 1D and 3D simulations. The 1D simulations tended to give unreliable results for cross-slope winds. The method based on the height at which the wind speed attains its maximum value showed less variation over certain ranges of wind direction relative to the orientation of the sloping surface.

Suggestions for future work include time-scale analysis of the mixing length to investigate how boundary layer turbulence is influenced by the introduction of a shallow slope.

5. ACKNOWLEDGEMENTS

S. H. Derbyshire's contribution is Crown Copyright 2007. The FORTRAN code for LES used in this paper was developed at the U.K. Meteorological Office by S.H.D. and co-workers. It is based on an original code of Dr P. J. Mason.

6. REFERENCES

BROWN A.R., S.H. DERBYSHIRE & MASON P.J. (1994). Large-eddy simulation of stable atmospheric boundary layers with a revised stochastic subgrid model. *Q. J. R. Meteorol. Soc.* 120, 1485-1512.

DERBYSHIRE, S.H. & N. WOOD (1994). The sensitivity of stable boundary layers to small slopes and other influences. *in:* I.P. Castro & N.J. Rockliff (Eds.) *Stably*

Stratified Flows: Flow and Dispersion over Topography. The Institute of Mathematics and its Applications Conference Series, Clarendon Press, Oxford. 105-118.

HANDORF D., T. FOKEN & C. KOTTMEIER (1999). The stable atmospheric boundary layer over an Antarctic ice sheet. *Boundary-Layer Meteorol.* 91(2), 165-189.

KAIMAL, J.C., R.A. EVERSOLE, D.H. LENSCHOW, B.B. STANKOV, P.H. KAHN & J.A. BUSINGER (1982). Spectral characteristics of the convective boundary layer over uneven terrain. *J. Atmos. Sci.* 39, 1098-1114.

KING J.C. (1990). Some measurements of turbulence over an Antarctic ice shelf. *Quart. J. R. Met. Soc.* 116, 379-400.

KOTTMEIER C. (1986). Shallow gravity flows over the Ekstrom Ice shelf. *Boundary-Layer Meteorol.* 35, 1-20.

MAGUIRE A.J., J.M. REES & S.H. DERBYSHIRE (2006). Stable atmospheric boundary layer over a uniform slope: some theoretical concepts. *Boundary-Layer Meteorol.* 120, 219-227.

MAHRT, L., D. VICKERS, R. NAKAMURA, M.R. SOLER, J. SUN, S. BURNS & D.H. LENSCHOW (2001). Shallow drainage flows. *Boundary-Layer Meteorol.* 101, 243-260.

MASON P.J. (1989). Large-eddy simulation of the convective atmospheric boundary layer. *J. Atmos. Sci.* 46, 1492-1516.

MASON P.J. & DERBYSHIRE S.H. (1990). Large-eddy simulation of the stably stratified atmospheric boundary layer. *Boundary-Layer Meteorol.* 53, 117-162.

PIACSEK S.A. & G.P. WILLIAMS (1970). Conservation properties of convection difference schemes. *J. Comp. Phys*. 6, 392-405.

REES, J.M. (1991). On the Characteristics of Eddies in the Stable Atmospheric Boundary Layer. *Boundary-Layer Meteorol.* 55, 325–343.

SKYLLINGSTAD, E.D. (2003). Large-eddy simulation of katabatic flows. *Boundary-Layer Meteorol.* 106, 217-243.

ZILITINKEVICH S.S. (1972). On the determination of the height of the Ekman boundary layer. *Boundary-Layer Meteorol.* 3, 141-145.